Modelling the influence of low concentrations of water on the thermodynamics, electron transfer kinetics and diffusivity of the $[Ru(CN)_6]^{4-/3-}$ process in propylene carbonate

Atul Sharma [a], Jiezhen Li [a], Si-Xuan Guo [a,b], Alan M. Bond [a,b,*] and Jie Zhang [a,b,*]

[a] *School of Chemistry, Monash University, Clayton, VIC,3800, Australia*

[b] *ARC Centre of Excellence for Electromaterials Science, Monash University, Clayton, VIC 3800, Australia*

alan.bond@monash.edu, jie.zhang@monash.edu

Abstract

Addition of low concentrations of water to an aprotic solvent can lead to large changes in the thermodynamics of some electrode processes. In contrast, the impact of water addition on the electrode kinetics of such systems has yet to be established. Herein, direct current and Fourier transformed alternating current voltammetric studies have been undertaken at a glassy carbon electrode to investigate changes in the thermodynamics, kinetics and diffusivity of the $[Ru(CN)_6]^{4-/3-}$ process in propylene carbonate (PC, 0.10 M *n*-Bu_4NPF_6) that occur on addition of up to 1.87 M water and in fully aqueous 0.10 M KCl electrolyte media. The formal reversible potential (E_f^0) for the $[Ru(CN)_6]^{4-/3-}$ couple is -0.66 V vs $Fc^{0/+}$ (Fc = ferrocene) in PC and shifts substantially in the positive direction by about 0.35 V in the presence of 1.87 M water, and is established to be 1.0 V more positive in fully aqueous media. In comparison, E_f^0 for the $Fc^{0/+}$ process only changes by approximately 20 mV vs a Pt quasi reference electrode in the presence of 1.87 M water, emphasising the impact of charge and structure on the thermodynamics. Modelling the water induced shift in E_f^0 in terms of solvent interaction implies that transfer of approximately four water molecules in the secondary coordination sphere accompanies the oxidation of $[Ru(CN)_6]^{4-}$ to $[Ru(CN)_6]^{3-}$. Despite the implied large level of solvent rearrangement, the heterogeneous electron charge transfer rate constant only increases from 1.81×10^{-2} cm s^{-1} in neat PC to 3.38×10^{-2} cm s^{-1} on addition of 1.87 M water to PC. An increase in diffusivity of $[Ru(CN)_6]^{4-}$ was observed but is not evident in the $Fc^{0/+}$ process under the same conditions, hence is probably not simply due to the small decrease in viscosity that occurs on addition of low concentrations of water. Some, but not all aspects of the kinetics are in qualitative agreement with Marcus theory predictions.

Keywords: $[Ru(CN)_6]^{4-/3-}$ process, propylene carbonate, thermodynamics, electron transfer kinetics, diffusivity, effects of water, voltammetry

1. Introduction

Quantitative voltammetric studies provide valuable insights into the thermodynamics and electrode kinetics of reaction mechanisms associated with electron transfer in chemical as well as biological systems [1-2]. For several decades, the thermodynamics of ruthenium-based redox couples in three common oxidation states (II, III, and IV) [3-4] has attracted significant attention due to widespread use of ruthenium in diverse fields such photovoltaic cells, medicinal chemistry, and catalysis [5-7]. With relevance to the present study, water-soluble alkali cyanoruthenate salts such as $K_4[Ru(CN)_6]$ and $K_3[Ru(CN)_6]$ have been shown to display well defined $[Ru(CN)_6]^{4-/3-}$ (Eq.1) voltammetry in aqueous electrolyte media [8] allowing the reversible formal potential (E_f^0) to be calculated in this solvent. However, electrode kinetic data are not available in water. Furthermore, neither thermodynamic or electrode kinetic data are available in organic solvents even though these media are important in the context of applications [9].

$$[Ru^{II}(CN)_6]^{4-} \rightleftharpoons [Ru^{III}(CN)_6]^{3-} + e^- \quad \textbf{(1)}$$

The effects of solvent on electron transfer processes associated with organometallic complexes and enzyme co-factors have also been extensively investigated [2, 10-18]. While there is a paucity of data related to the $[Ru(CN)_6]^{4-/3-}$ process in organic solvents, the impact of variation of solvent on E_f^0 for other ruthenium redox couples has been of interest for many years [19-21]. For example, the electrochemistry of the dinuclear $\{[Ru(CN)_4]_2(\mu\text{-bppz})\}^{4-}$ complex (bppz = 2,3-bis(2-

64 pyridyl)pyrazine) as a water-soluble (K^+) salt and dichloromethane soluble PPN^+ salt (PPN^+ =
65 bis(triphenyl-phosphino)iminium cation) has been shown to display strong solvent-dependent
66 behaviour when changing from water to dichloromethane [20]. It also has been established that the
67 E_f^0 for the $[Ru(bipy)(CN)_4]^{2-/3-}$ couple (bipy = bipyridine) is several hundred mV more positive in
68 water than in organic solvents [20, 22-23]. This solvent-dependent variation in E_f^0 and indeed in
69 spectroscopic properties of related compounds [24] has been attributed to electrostatic interaction of
70 this solvent with the ligand, hydrogen bonding ability of the water molecule, and differences in the
71 supporting electrolyte. In recent years, Density Functional Theory (DFT) studies also have been
72 used to predict Ru(II/III) redox potentials [25-28].

73 The present study reports a thermodynamic and kinetic study of the $[Ru(CN)_6]^{4-/3-}$ process
74 derived from analysis of the DC and AC voltammetry in propylene carbonate (PC) in the absence
75 and presence of up to 1.87 M water and in fully aqueous 0.10 M KCl electrolyte media. The
76 thermodynamics of the $[Ru(CN)_6]^{4-/3-}$ process are quantified by the values of E_f^o as a function of
77 water concentration. The electron transfer kinetics are parameterised by determining the values of
78 the heterogeneous electron transfer rate constant (k^0) at E_f^o and the electron transfer coefficient
79 (α), using the Butler-Volmer relationship [29-30], again as a function of water concentration. E_f^o for
80 the $[Ru(CN)_6]^{4-/3-}$ process in PC is highly sensitive to the presence of small concentrations of water
81 as applies to the related $[Fe(CN)_6]^{3-/4-}$ process [31]. In contrast, the k^0 values, even though calculated
82 at E_f^o, change relatively little on the addition of water. This minimal electrode kinetic effect may
83 be regarded as surprising since the impact of water on the thermodynamics implies substantial
84 solvent reorganisation accompanying the oxidation of $[Ru(CN)_6]^{4-}$ to $[Ru(CN)_6]^{3-}$, which in

principle slows down the rate of an electron transfer process [30] according to the Marcus-Hush theory [32-33].

2. Experimental

2.1 Chemical reagents: Potassium hexacyanoruthenate(II) hydrate ($K_4[Ru(CN)_6]\bullet 3H_2O$, Sigma Aldrich), tetramethylammonium hydroxide pentahydrate ($Me_4N(OH)\bullet 5H_2O$, ≥97%, Sigma), hydrochloric acid (32%, Ajax finechem) and ethanol (99.5%, Ajax finechem), methanol (99.8 %, Sigma-Aldrich), isopropyl alcohol (Sigma-Aldrich) were used as received from the manufacturers. The supporting electrolyte *n*-tetrabutylammonium hexafluorophosphate (*n*-Bu_4NPF_6, 98.0 %, Wako) was recrystallized twice from ethanol. Propylene carbonate (PC, 99.7 %, Sigma) was purified and dried using standard procedures [34]. Briefly, the PC was percolated through molecular sieves (3 Å, activated at 350 ºC), transferred to an activated alumina containing air-tight container and stored in a glove box, when not in use. Ferrocene (Fc, ≥98%, Aldrich) was recrystallized from n-pentane (Merck). The water concentration in PC was determined by Karl Fisher titration using a Metrohm 831 KF coulometer. In "dry" PC, the water content was ≤130 ppm (≈ 0.01 M).

2.2 Synthesis of $(Me_4N)_4[Ru(CN)_6]$: Since the $K_4[Ru(CN)_6]$ salt is insoluble in PC, $(Me_4N)_4[Ru(CN)_6]$ was used to provide a PC soluble salt as needed for electrochemical studies in this solvent. To synthesize $(Me_4N)_4[Ru(CN)_6]$, the acid $H_4[Ru(CN)_6]$ was initially prepared from $K_4[Ru(CN)_6]$ as described in the literature [35]. Briefly, 50.0 mM (0.021g) $K_4[Ru(CN)_6]$ was dissolved in 0.10 M HCl (1.50 mL). Upon shaking this solution with diethyl ether (1:3 ratio), an etherate of the acid was precipitated. The etherate was then re-precipitated three times after dissolution in ethanol followed by addition of excess of diethyl ether. Ether free $H_4[Ru(CN)_6]$ was

collected by drying overnight at room temperature. The percentage yield was calculated as 82-84%. Finally, $(Me_4N)_4[Ru(CN)_6]$ was synthesized by mixing a 0.10 M $H_4[Ru(CN)_6]$ solution in isopropyl alcohol (1.50 mL) with 0.50 M $Me_4N(OH)$ in methanol (1.50 mL). The precipitate formed was collected by centrifugation and dried overnight under vacuum. Finally, the solid was thoroughly washed with water, recrystallized three times from ethanol and dried extensively before use. The yield based on the formula $(Me_4N)_4[Ru(CN)_6]$ was 75-78%. However, elemental analysis showed that solvent molecules of crystallization are present as commonly found for this kind of ruthenium compound [9]. Consequently, the concentration of $[Ru(CN)_6]^{4-}$ in solution was determined by a combination of steady state and transient cyclic voltammetry as described in detail in Section 2.3.

The preparation of $(Me_4N)_4[Ru(CN)_6]$ was monitored by infrared (IR) vibrational spectra at each step in the synthesis (Fig. S1)**.** The IR spectrum of $K_4[Ru(CN)_6]$ contained -CN asymmetric (ν_{as}) and symmetric (ν_s) bands at 2033 and 2051 cm^{-1}, respectively [36]. After protonation to form $H_4[Ru(CN)_6$, the -CN bands shifted +45 cm^{-1} and appeared at 2075 and 2099 cm^{-1} in the cyanide stretching region[36-37]. After reaction to form the Me_4N^+ salt, IR bands from tetramethyl (ν_{as} and ν_s, $-CH_3$) were detected between 2900-3040 cm^{-1} with their bending vibrations at 1479 and 1487 cm^{-1}, respectively. A strong vibrational band corresponding to -CN stretching (ν_{as} and ν_s) at 2032 cm^{-1} with a shoulder at 2027 cm^{-1} also was present as was a weak band corresponding to the bending vibration of the CN-Ru bond (δ C-N-Ru) at 662 cm^{-1} [38]. Tetraethylammonium and tetraphenylphosphonium hexacyanoruthenate(II) and other related salts[9, 35] exhibit similar IR spectral characteristics.

2.3 Voltammetric instrumentation and procedures: DC cyclic voltammetric measurements were undertaken in a standard three electrode electrochemical cell using a CHI 760E electrochemical workstation (CH Instruments, Texas, USA). The glassy carbon (GC) working electrode employed in transient cyclic voltammetric experiments had a nominal diameter of 1.0 mm (eDAQ). For steady state voltammetric measurements, a 10.0 μm diameter platinum microdisk working electrode (CH Instruments, Texas, USA) was used. Prior to each measurement, the working electrode was polished with an aqueous Al_2O_3 slurry (0.30 μm), rinsed consecutively with water and acetone and dried under N_2. A Pt wire was used as the counter electrode. For voltammetric studies in propylene carbonate in the presence of up to 1.87 M water, a Pt wire was used as the quasi-reference electrode. This Pt wire was inserted into a glass tube containing a 0.10 M Bu_4NPF_6 PC solution separated from the analyte solution by a porous glass frit. For voltammetric studies in aqueous electrolyte medium, Ag/AgCl (1.0 M KCl) was used as the reference electrode, with Pt wire again being used as the counter electrode. The supporting electrolyte in PC with and without added water was 0.10 M Bu_4NPF_6, and 0.10 M KCl for studies in the fully aqueous medium. Potentials in PC media vs the Pt quasi-reference electrode were corrected to the IUPAC recommended $Fc^{0/+}$ scale,[39] which was achieved using E_f^0 for the $Fc^{0/+}$ process determined from the cyclic voltammetry for oxidation of 0.25 mM Fc as either an internal[40] or external reference. The former was used in potential determinations, while the latter was used in kinetic studies to avoid any possible interference. Correction to the $Fc^{0/+}$ scale in an aqueous medium was achieved by subtracting 401 mV from the value measured vs Ag/AgCl [41]. All voltammetric studies were carried out at 20 ± 2 ºC.

148 To minimize contamination from atmospheric water, all solutions were prepared in a glove box
149 and sealed. The solutions were also pre-saturated with nitrogen. Oxygen was removed by purging
150 with N_2 for at least 20 min before each measurement. The effective electroactive area (A) of the
151 GC working electrode of 8.30×10^{-3} cm^2 was determined by relating the peak current (I_p) for
152 oxidation of 1.0 mM Fc in CH_3CN (0.10 M n-Bu_4NPF_6) to the Randles-Sevcik relationship (Eq.2)
153 [30] using the known diffusion coefficient (D_{Fc}) of 2.4×10^{-5} cm^2 s^{-1} for Fc under these conditions
154 [42].

155 $$I_P = 0.4463nFA\left(\frac{nFDv}{RT}\right)^{1/2} C \qquad \textbf{(2)}$$

156 In Eq.2, n is the number of electrons transferred (1.0), C is the bulk concentration, v is the scan
157 rate, D is the diffusion coefficient, T is the absolute temperature, F is Faraday's constant and R is
158 the universal gas constant.

159 The values of D and C for $[Ru(CN)_6]^{4-}$ in neat PC and in the presence of up to 1.87 M water were
160 calculated by solving the simultaneous equations derived from the steady-state limiting current
161 (I_{ss}) [43] (Eq.3) at the Pt-microdisk electrode (radius r = 5.0 μm) at a scan rate of 10.0 mV s^{-1} and
162 the peak current obtained at the GC macrodisk electrode at a scan rate of 100 mV s^{-1} using the
163 Randles-Sevcik relationship (Eq.2) (assuming the $[Ru(CN)_6]^{4-/3-}$ process is reversible). The use of
164 this approach to calculate $D_{[Ru(CN)_6]^{4-}}$ and C was to eliminate possible uncertainty arising from
165 the presence of solvate in the $(Me_4N)_4[Ru(CN)_6]$ salt used as the source of $[Ru(CN)_6]^{4-}$, noting that
166 solvates are present in X-Ray crystallographic structures reported for both $[Ru(CN)_6]^{4-}$ and
167 $[Ru(CN)_6]^{3-}$ salts [9].

168 $I_{ss} = 4\,nFDCr$ **(3)**

169 In this equation, I_{ss} and r denote the steady-state mass transport limiting current and radius of the
170 microdisk electrode, respectively.

171 The value of $D_{[Ru(CN)_6]^{4-}}$ in water (0.10 M KCl) was determined from measurement of I_p for
172 oxidation of $[Ru(CN)_6]^{4-}$ by DC voltammetry at the GC electrode as a function of $v^{1/2}$ and use of
173 the Randles-Sevcik equation. $D_{[Ru(CN)_6]^{4-}}$ and $D_{[Ru(CN)_6]^{3-}}$ were assumed to be equal in
174 simulations of the voltammetry.

175 Fourier transformed alternating current (FTAC) voltammetry experiments were undertaken using
176 in-house built instrumentation [44-45] with an applied sine wave perturbation having an amplitude
177 (ΔE) of 80 mV and a frequency (f) of 9.02 or 80.99 Hz, superimposed onto the DC ramp. The cell,
178 electrodes and other conditions were the same as for DC voltammetry. FTAC voltammetric data
179 obtained from either experiment or simulation in the time domain were converted to the frequency
180 domain to generate the power spectrum [46-47]. Frequencies corresponding to the AC harmonics and
181 DC component were selected from the power spectrum and then subjected to band filtering and
182 inverse Fourier transform to obtain resolved DC and AC components.

183 **2.4: Other instrumentation**: IR spectra were recorded with a Cary 630 FTIR spectrometer in the
184 attenuated total reflectance mode over the range of 4000 to 600 cm^{-1} at room temperature using
185 128 scans at a resolution of 32 cm^{-1} under vacuum conditions.

2.5 Simulations: FTAC voltammetric data were simulated with the Monash Electro-Chemistry Simulator (MECSim) software package (http://www.gareth kennedy.net/MECSim.html) [48]. To model the one-electron transfer process (Eq. 4), the Butler-Volmer formalism [29] was used.

$$R \rightleftharpoons O + e^- \qquad (E_f^0, k^0, \alpha) \qquad \textbf{(4)}$$

In Eq.4, R and O are the reduced ($[Ru(CN)_6]^{4-}$) and oxidised ($[Ru(CN)_6]^{3-}$) forms of the electroactive species respectively described in Eq.1. In the simulations, in addition to E_f^0, k^0, α, that need to be estimated, other parameters such as R_u (uncompensated resistance), C_{dl} (double layer capacitance), A and D are required as inputs for the MECSim software. Some of these parameters were determined independently. The average of the oxidation (E_P^{ox}) and reduction (E_P^{red}) peak potentials in DC cyclic voltammogram provided an estimate of E_f^0, which was used as input in the heuristic form of data analysis. R_u was determined from the R_uC_{dl} time constant at a potential where no faradaic current was present [49]. C_{dl} was calculated from background current associated with the fundamental harmonic modelled in terms of a non-linear (Eq.5) capacitor as suggested by Tokuda and Matsuda [49-50] in the potential range where faradaic current is absent. Herein, the non-linear capacitance is defined by the coefficients c_0, c_1, c_2, c_3 and c_4, and time dependent potential is designated by $E(t)$.

$$C_{dl}(t) = c_0 + c_1E(t) + c_2E(t)^2 + c_3E(t)^3 + c_4E(t)^4 \qquad \textbf{(5)}$$

In the initial heuristic form of data analysis, comparisons of AC harmonic components derived from experimental and simulated data were undertaken by the experimenter to obtain k^0 and α values, with E_f^0 treated as a known parameter. In this approach, the experimenter varied k^0 and α

values in the simulations until the "best fit" was achieved by visual comparison with the experimental data. Clearly, this represents a tedious and time-consuming exercise even when E_f^0 is fixed and only k^0 and α varied. However, the outcome provided the basis for limiting the range of E_f^0, k^0, and α values to be searched by the computationally intensive data optimisation approach. In this method, MECSim script was encoded on Python encrypt [51]. In the Python encrypted Docker operating system, the parameters to be estimated were selected in the input file (Master.sk) and their range to be searched was input in RandomlySampleRange.ipynb for each variable and based on the estimations made in the preliminary heuristic form of data analysis. The resolution typically chosen for searching the E_f^0, k^0, α parameter space was 1.0 mV, 0.01 cm s^{-1} and 0.01, respectively. In this manner, simulated data based on many combinations of parameters within the specified range and resolution could be calculated and compared computationally with the experimental data on a laptop computer to obtain the best fit.

An algorithm based on python encrypted Docker software operating system was used to generate the envelope of the AC data for each AC harmonic component and this form of data was used for comparison of experimental and simulated data. CompareSmoothed.ipynb sub-script was used to compare the experimental and simulated data with the RandomlySampleRange.ipynb and HarmonicSplitter.ipynb Python sub-scripts was used to simulate and display the comparison of the data for every simulated combination of E_f^0, k^0, α parameters. The difference between experimental and simulated data is described by the least squares function (LS) (Eq.6) in the form of a percentage. In this study, the DC and fundamental harmonic components were excluded from the calculation of LS due to imperfect modelling of the background current that is prominent in these components, but essentially absent in second and higher order kinetically very sensitive AC

harmonics. Full details of the MECSim supported automated data optimization protocol are described elsewhere (http://www.garethkennedy.net/MECSimDownload.html).

$$\mathrm{LS} = \left[1 - \frac{1}{H-1}\left(\sum_{h=2}^{H}\sqrt{\frac{\sum_{i=1}^{N}[(f_h^{exp}(x_i) - f_h^{sim}(x_i))^2]}{\sum_{i=1}^{N} f_h^{exp}(x_i)^2}}\right)\right] \times 100\% \qquad \textbf{(6)}$$

In the expression for LS in Eq.6, $f^{\mathrm{exp}}(x_i)$ and $f^{\mathrm{sim}}(x_i)$ represent the experimental and simulated functions, respectively and h (= 2 to H) represents the relevant AC harmonic, H is the total number of AC harmonic components and N is the number of data points.

3. Results and Discussion

3.1 DC cyclic voltammetry for the oxidation of $[Ru(CN)_6]^{4-}$ to $[Ru(CN)_6]^{3-}$

The $[Ru(CN)_6]^{4-/3-}$ process was initially characterized by DC cyclic voltammetry at a GC electrode. In the analysis of data derived from these experiments, E_f^o was equated with the midpoint potential (average of the oxidation (E_P^{ox}) and reduction (E_P^{red}) peak potentials) and hence from ($E_P^{ox} + E_P^{red}$)/2, and the peak-to-peak separation ΔE_p from the difference in E_P^{ox} and E_P^{red}. Fig. 1(a) displays a DC cyclic voltammogram obtained with a GC electrode using a scan rate of 100 mV s^{-1} for oxidation of 0.083 mM $[Ru(CN)_6]^{4-}$ in PC (0.10 M *n*-Bu_4NPF_6). The cyclic voltammograms obtained for the $[Ru(CN)_6]^{4-/3-}$ process in PC with a GC electrode over the scan rate range from 50 to 500 mV s^{-1} (Fig. S2) gave ΔE_p values in the range of 75 to 100 mV as predicted for a quasi-reversible process and a scan rate independent value of -0.66 V vs $Fc^{0/+}$ for $E_{f,PC}^0$. In contrast, cyclic voltammetry for the $[Ru(CN)_6]^{4-/3-}$ process in an aqueous media containing 0.10 M KCl as the

supporting electrolyte (Fig. S3) gave E^0_{f,H_2O} = 0.34 V vs $Fc^{0/+}$ which is 1.00 V more positive than $E^0_{f,PC}$ in PC (0.10 M *n*-Bu_4NPF_6).

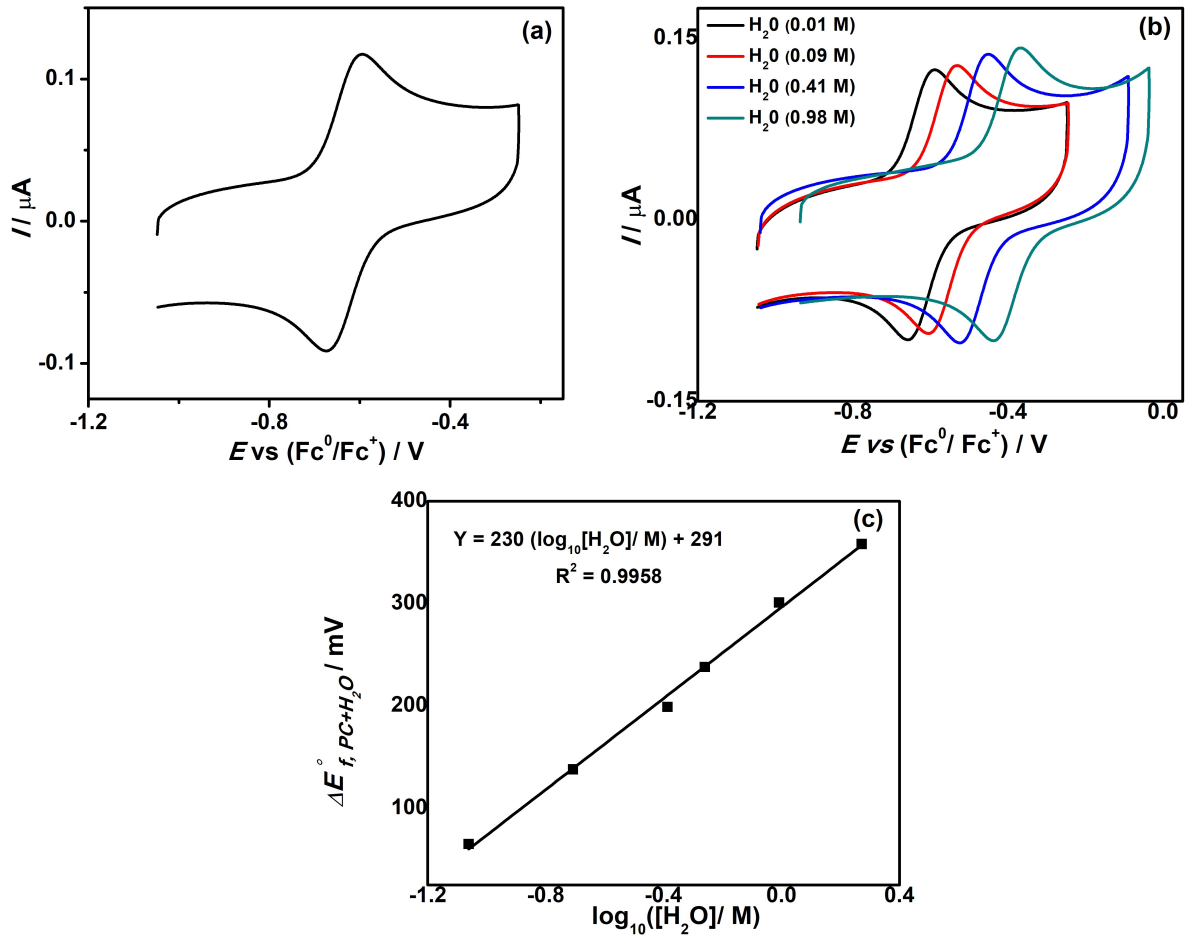

Figure 1: DC cyclic voltammograms obtained at a GC electrode in PC (v = 100 mV s^{-1}) containing 0.10 M *n*-Bu_4NPF_6 as supporting electrolyte for oxidation of 0.083 mM $[Ru(CN)_6]^{4-}$ (a) without water and (b) with designated water concentrations. (c) the shift in $\Delta E^0_{f,PC\ \ H_2O}$ for the $[Ru(CN)_6]^{4-/3-}$ process as a function of water concentration.

The $D_{[Ru(CN)_6]^{4-}}$ values in PC (0.10 M *n*-Bu_4NPF_6) and aqueous 0.10 M electrolyte, along with other parameters relevant to the DC voltammetry in these media are summarised in Table 1. The diffusion coefficient is governed by the Stokes-Einstein relationship (Eq.7) [52]

$$D = k_B T / 6\pi\eta a \quad \textbf{(7)}$$

where, k_B is the Boltzmann constant, η is the viscosity of the solvent and a is the hydrodynamic radius of the diffusing species. According to Eq.7, D depends upon viscosity, so the smaller value in PC (η = 2.50 cP, , 0.01 M H_2O) of 1.91 × 10^{-6} cm^2 s^{-1} relative to the value of 6.91×10^{-6} cm^2 s^{-1} in water (η = 0.89 cP) is as expected. A D value of 7.46 × 10^{-6} cm^2 s^{-1} for $[Ru(CN)_6]^{4-}$ in aqueous medium (0.10 M $LiClO_4$) was determined by O'Mullane et al using a Pt ultramicroelectrode [53]. In the present work, D_{Fc} in PC (0.01 M H_2O) in the presence of 0.10 M *n*-Bu_4NPF_6 was found to be 3.28 ± 0.06 × 10^{-6} cm^2 s^{-1} based on the DC voltammetry for the oxidation of Fc using Eq.2 and the steady state mass transport limiting current using Eq.3. A literature value is 5.6 × 10^{-6} cm^2 s^{-1} in a PC (0.14 M H_2O) in presence of 0.10 M $LiClO_4$ at GC (diameter 2.7 mm) electrode [54]. Janisch et al [55] in a very detailed study noted that the incorporation of incorrect value of either the electrode area or radius can lead to significant errors in the determination of the diffusion coefficient, but reported a D_{Fc} value of 4.0 × 10^{-6} cm^2 s^{-1} in PC (0.14 M H_2O) after careful analysis of data obtained with a 10.0 µm diameter Pt microelectrode. In summary, D values for both $[Ru(CN)_6]^{4-}$ and Fc obtained in the present work are in satisfactory agreement with literature values, but as noted by Janich et al, variation in the literature on reports of this parameter are often substantial for unknown reasons.

Table 1: Comparison of *D* values at 20 ºC derived from the oxidation of 0.083 mM $[Ru(CN)_6]^{4-}$ in PC (0.10 M *n*-Bu_4NPF_6) and 0.94 mM of $[Ru(CN)_6]^{4-}$ in aqueous media (0.10 M KCl) at a scan rate of 100 mV s^{-1}.

Salt used as source of $Ru(CN)_6]^{4-}$	**Solvent (η/cP at 20 ºC)**	**Electrolyte (0.10 M)**	E_f^0 ***vs*** **$Fc^{0/+}$ (V)**	***D*** **(10^{-6} cm^2 s^{-1})**
$[(Me_4)N]_4[Ru(CN)_6]$	PC (2.50)	*n*-Bu_4NPF_6	-0.66	1.91 ± 0.03
$K_4[Ru(CN)_6]$	Water (0.89)	KCl	0.34	6.91 ± 0.05

The dependence of the DC cyclic voltammetry for the $[Ru(CN)_6]^{4-/3-}$ process in PC on addition of water up to a final concentration of 1.87 M is shown in Fig. 1b. The positive potential shifts ($\Delta E^0_{f,PC+H_2O} = E^0_{f,PC+H_2O} - E^0_{f,PC}$) in reversible potential upon addition of water ($E^0_{f,PC+H_2O}$) with respect to that in neat PC ($E^0_{f,PC}$) are summarised in Table 2, where $E^o_{f,PC+H_2O)}$ values are reported vs the $Fc^{0/+}$ scale which is assumed to be independent of water concentration.

Table 2: Summary of data obtained by DC cyclic voltammetry at a GC electrode using a scan rate of 100 mV s^{-1} for the oxidation of 0.083 mM $[Ru(CN)_6]^{4-}$ in PC (0.10 M *n*-Bu_4NPF_6) containing designated concentrations of water.

Water conc. (M)	η (cP)*	I_p^{ox} (μA)	D (10^{-6} cm^2 s^{-1})	$E^0_{f,PC+H_2O}$ vs $Fc^{0/+}$ (V)	$\Delta E^0_{f,PC+H_2O}$ (mV)	ΔE_p (mV)
0.01	2.50	0.081	1.91	-0.656	0	84
0.09	2.48	0.085	2.06	-0.588	68	79
0.20	2.46	0.087	2.18	-0.526	130	77
0.41	2.40	0.090	2.36	-0.464	192	74
0.55	2.38	0.091	2.39	-0.430	226	73
0.98	2.31	0.095	2.59	-0.364	292	72
1.87	2.22	0.100	2.80	-0.302	354	71

* values taken from reference [56] for the electrolyte free PC and H_2O mixtures.

The dependence of a range of other parameters on water concentrations also is provided in Table 2. The ΔE_p value of 84 mV obtained at a GC electrode (Table 2) in the absence of water is consistent with a moderately slow $[Ru(CN)_6]^{4-/3}$ electron transfer process. ΔE_p in PC/water mixtures then decreases from 84 to 71 mV in the presence of 1.87 M water implying that k^0 increases on addition of water. In pure water, ΔE_p is 62 mV which approaches the value of 57 mV predicted for a reversible process at 20 °C. Thus, addition of water also has electrode kinetic and diffusivity effects which will be quantified by studies presented below.

Although relatively small amounts of water added to PC induce a large thermodynamic effect (Figure 1), DC voltammetric data reveal that while $D_{[R_u(CN)_6]^{4-}}$ increases progressively as water is added up to a final concentration of 1.87 M (Table 2), the impact on the diffusivity (mass transport) is relatively small by comparison. However, while the trend for the $D_{[R_u(CN)_6]^{4-}}$ change is in agreement with the viscosity data given in Table 2[56], the increase is significantly greater than

predicted by the Stokes-Einstein relationship (Eq.7). Further discussion on the dependence of diffusivity data on water concentration is provided below.

It is informative to compare data obtained from DC cyclic voltammetry for the $[Ru(CN)_6]^{4-/3-}$ process as described above and the $Fc^{0/+}$ process in PC in the presence of up to 1.87 M water. The $\Delta E^0_{f,PC\ \ H_2O}$ value for $[Ru(CN)_6]^{4-/3-}$ process shifted by about 350 mV and the value of $D_{[Ru(CN)_6]^{4-}}$ from 1.91 to 2.80 × 10^{-6} cm^2 s^{-1} (Table 2) in the presence of 1.87 M water. In contrast, no significant impact was noted on $E^o_{f,Fc}$ and D_{Fc} values (Table 3). That is, E^o_f for the $Fc^{0/+}$ process did not vary significantly vs the Pt quasi-reference (Table 3), which is analogous to the finding reported by Noftle and Pletcher [31], who found that the potential for the $Fc^{0/+}$ process vs the saturated calomel electrode is almost independent of addition of up to 2.40 M water to PC and 10.20 M water to acetonitrile.

Table 3: Summary of data obtained by dc cyclic voltammetry at a GC electrode using a scan rate of 100 mV s^{-1} for the oxidation of 0.25 mM Fc in PC (0.10 M *n*-Bu_4NPF_6) containing designated concentrations of water.

Water conc. (M)	D **(10^{-6} cm^2 s^{-1})**	$E^0_{f,PC+H_2O}$ ***vs*** $Fc^{0/+}$ **(V)**	$\Delta E^0_{f,PC+H_2O}$ **(mV)**	ΔE_p **(mV)**
0.01	3.28	0.647	0	62
0.09	3.26	0.644	-3	61
0.20	3.28	0.641	-6	63
0.41	3.32	0.639	-8	61
0.55	3.33	0.634	-13	64
0.98	3.30	0.636	-11	63
1.87	3.29	0.634	-13	61

322

323 Traditionally, when rationalising the solvent dependence of spectroscopic parameters, the relevant
324 donor and acceptor properties of the solvents are considered. With respect to the solvents, the
325 relative strengths of the electron accepting properties are commonly quantified by reference to the
326 Gutmann donor-acceptor number [57]**.** Water is a class of its own in terms of the Gutmann acceptor
327 number having a very large value of 54.8, while PC is a relatively poor electron acceptor with a
328 Gutmann donor number of 18.3 [57-58]**.** This combination of large and small Gutmann donor-acceptor
329 number in water and PC respectively can account for the very large 1.0 V difference in E_f^o provided
330 that the impact is highly dominant in the reduced $[Ru^{II}(CN)_6]^{4-}$ form relative to the oxidised
331 $[Ru^{III}(CN)_6]^{3-}$ one.
332 In the case of the $[Ru(CN)_6]^{4-/3-}$ redox system, large positive differences in E_f^o in water relative to
333 PC can be attributed to enhanced dipolar interaction of the complex $[Ru^{III}(CN)_6]^{3-}$ anion in water
334 and stronger interaction with lone pairs of electrons on the cyanide ligands in $[Ru^{II}(CN)_6]^{3-}$ as
335 electron acceptors relative to $[Ru^{III}(CN)_6]^{4-}$, principally via hydrogen bonding with H atoms acting
336 as the electron acceptors[23-24]. This electron-accepting behaviour of the solvent is quantified by the
337 Gutmann acceptor number. Strong interaction also has been found in the solid state where for
338 example in the structure of $Ph_4P_3[Ru^{II}(CN)_6]\cdot 2(i\text{-PrOH})$, it was found that some of the cyanide
339 ligands are hydrogen bonded to 2-propanol [9]. Furthermore, in solid $H_4[Ru^{II}(CN)_6]^{4-}$ all four
340 hydrogen atoms are involved in hydrogen bonding to the cyanide ligand [26], and in the related
341 $Ph_4P_3[Os^{II}(CN)_6]\cdot 3CH_2Cl_2\cdot 2H_20$, the cyanide ligands are bonded to water [9].
342 A schematic representation of the structures of $K_4[Ru^{II}(CN)_6]$, water and PC are provided in Fig.
343 2. Fig. 3a represents the flow of electron in the ruthenium cyanide system upon interaction with

an electron acceptor. [57] The hydrogen bonding interaction of $[Ru^{II}(CN)_6]^{4-}$ with water is displayed in Fig. 3b. Fig. 3 displays how cyanide ligands with high basicity can donate electron density to hydrogen atoms of a water molecule. The donor properties of the nitrogen atoms of cyanoruthenate(II) are much stronger than cyanoruthenate(III) because the Ru(II) is a weaker electron acceptor and a stronger π electron donor. Hence, an increase in the acceptor properties of solvent results in an increase in the reversible potential associated with the $[Ru(CN)_6]^{4-/3-}$ process.

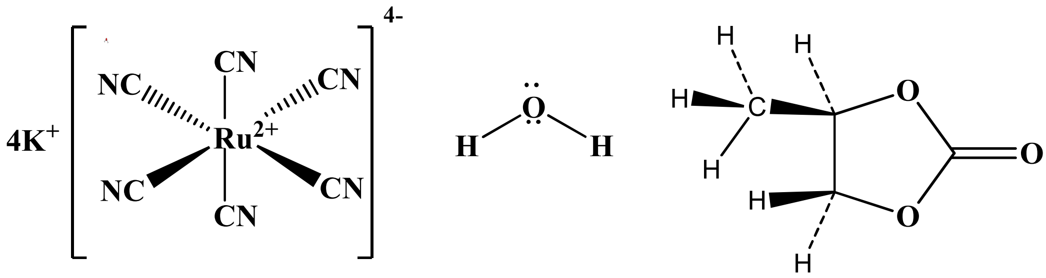

(a) (b) (c)

Figure 2: Structures of (a) potassium hexacyanoruthenate(II), (b) water and (c) propylene carbonate (PC).

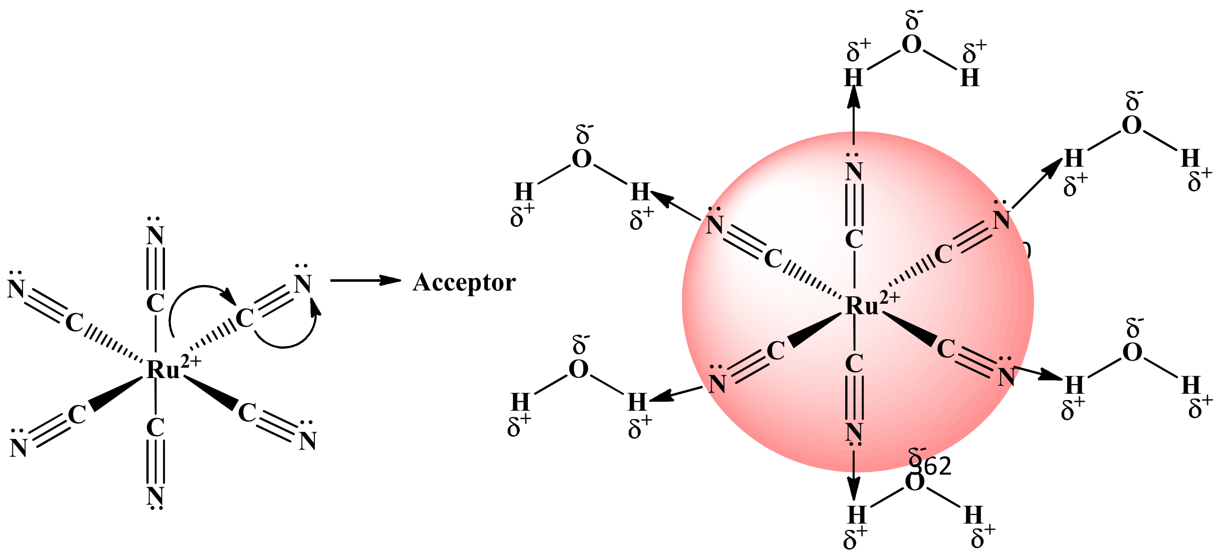

(a) (b)

364 **Figure 3: (a)** Representation of donor-acceptor interaction, **(b)** electrostatic interaction between
365 $[Ru(CN)_6]^{4-}$ and water.

366

367 Gutmann and co-workers [57, 59-61] have discussed the influence of solvent on E_f^o for the $[Fe(CN)_6]^{4-}$
368 $^{/3-}$ process in terms of the acceptor properties of the solvent. Their results demonstrated that the
369 influence of solvent is often large and in the seven aprotic solvents investigated, the value of E_f^o
370 was more negative than in water by 1.0-1.3 V, as now found in the related $[Ru^{II}(CN)_6]^{4-/3-}$ process
371 in the PC vs water comparison.

372 Based on what the authors regarded as important and often overlooked results provided by
373 Gutmann et al [57, 59-60], Noftle and Pletcher [31] restudied and confirmed the very positive potential of
374 the $Fe(CN)_6]^{3-/4-}$ process in water relative to that in PC and CH_3CN. They suggested a quantitative
375 interpretation for modelling the dependence of E_f^o in organic solvent-water mixtures on the water
376 concentration. At the height of the polarographic era, studies on ligand complexation within the
377 primary coordination sphere of metal ions were extensive [62]. Commonly, equilibrium constants
378 calculated from equations relating to the half-wave potential at a dropping mercury electrode [62-63],
379 as a function of the ligand concentration. Noftle and Pletcher adopted this formalism and treated
380 water as a ligand added to the secondary coordination sphere.[31] In the present study, this requires
381 treating the $[Ru(CN)_6]^{4-/3-}$ reaction as a square reaction scheme described in Eq.8 and
382 parameterising the relationship *via* use of Eq.9 assuming water complexation processes to be
383 reversible. This is a good approximation, provided the rate of electron transfer is fast. A recent
384 study suggests that discrepancies between theory and experiment may emerge when the electron

transfer process is slow and hence significant departs from reversible are evident in the voltammetry.[64] Eq. 10 was derived on the basis of the square reaction scheme (Eq. 8).[62]

$$[Ru^{II}(CN)_6]^{4-} \cdot qH_2O \rightleftharpoons [Ru^{III}(CN)_6]^{3-} \cdot pH_2O + (q - p)\, H_2O + e^-, \quad \text{where } q > p. \qquad \textbf{(8)}$$

$$\begin{array}{ccc} [Ru^{III}(CN)_6]^{3-} + e^- & \rightleftharpoons & [Ru^{II}(CN)_6]^{4-} \\ pH_2O \;\Big\uparrow\Big\downarrow\; K_{III} & & qH_2O \;\Big\uparrow\Big\downarrow\; K_{II} \\ [Ru^{III}(CN)_6]^{3-} \cdot pH_2O + (q - p)\, H_2O + e^- & \rightleftharpoons & [Ru^{II}(CN)_6]^{4-} \cdot qH_2O \end{array} \qquad \textbf{(9)}$$

$$\Delta E_f^0 = E^0_{f,PC+H_2O} - E^0_{f,PC} = 2.303RT/F \{\log_{10}(K_{II}/K_{III}) + (q - p) \log_{10}[H_2O]\} \qquad \textbf{(10)}$$

In Eqs. 9 and 10, K_{II} and K_{III} represent the overall stability constants for the association of q molecules of water with ruthenium(II) hexacyanide and p molecules of water with ruthenium(III) hexacyanide, respectively.

Fig. 1c displays the plot of $\Delta E^0_{f,PC+H_2O}$ for the $[Ru(CN)_6]^{4-/3-}$ process vs log([H_2O]/M). The data were fitted to a linear equation (Eq.10) [63] with a correlation coefficient of $R^2 = 0.9958$, a slope of 230 and an intercept of 291. On this basis, the value of (q-p) is approximately 4 and the stability constant ratio (K_{II}/K_{III}) is 7.14×10^4. Values of ($p - q$) and K_{II}/K_{III} were calculated to be 6.2 and 3.5 $\times 10^8$ M for the $[Fe(CN)_6]^{3-/4-}$ process respectively when up to 2.50 M water was added to acetonitrile[31]. These results imply that stronger interaction of water occurs with $[Fe(CN)_6]^{3-}$ than with $[Ru(CN)_6]^{3-}$ and that approximately six water molecules are transferred in the secondary coordination sphere when $[Fe(CN)_6]^{4-}$ is oxidised to $[Fe(CN)_6]^{3-}$ versus four when $[Ru(CN)_6]^{4-}$ is oxidised to $[Ru(CN)_6]^{3-}$.

In the above discussion, specific interaction of $[Ru(CN)_6]^{4-}$ and $[Ru(CN)_6]^{3-}$ with PC has been neglected. This is on the basis that PC has a much larger dipole moment of 4.81 D than water (1.86 D) [65], implying that presence of positive charge on all hydrogen atoms, the negative charge on the carbonyl group and the methyl group in side chain [66] favour cation-solvent interaction over an anion-solvent interaction. Indeed, whilst substantial changes are detected in the $[Ru(CN)_6]^{4-/3-}$ process in PC on addition of small concentrations of water, the addition of PC to a fully aqueous 1.0 mM $[Ru(CN)_6]^{4-}$ solution has virtually no impact on the process according to the DC voltammetric data shown in Fig.S4.

Due to the presence of highly negative charges on $[Ru(CN)_6]^{4-}$ and $[Ru(CN)_6]^{3-}$, ion-pairing with the electrolyte cation, Bu_4N^+, must be present and in principle should be included in the square reaction scheme. That is Eq. 10 should be replaced by an equation that takes into accounts both ion-pairing and solvent effects.[67] However, on increasing the electrolyte concentration from 0.10 to 0.50 M *n*-Bu_4NPF_6 in PC, a positive shift of only 24 mV in $E^0_{f,PC}$ was observed which is significantly smaller than that of about 160 mV calculated using the equation given in the inset to Fig. 1c when the concentration of water is increased from 0.10 to 0.50 M. On the basis that water solvent effect is dominant, ion-pairing effect was omitted in data analysis.

In studies with other redox couples, solvent and hydrogen bonding interactions also have been concluded to play an important role in determining the E^0_f value with the entropy as well as the enthalpy contributions to the free energy change (related to E^0_f) considered [68]. On addition of a polar solvent to an aprotic one, the positive shift in E^0_f has been correlated with hydrogen bonding interactions analogous to those occurring with the $[Ru(CN)_6]^{4-/3-}$ process in PC on addition of

water. For example, the effect of water on the reduction of stilbenes in dimethylformamide [69], hydrogen bonding and protonation effects on the electrochemistry of quinones in aprotic solvents [70], the effect of water on the electrochemistry of cytochrome c in dimethyl sulfoxide [68], and the influence of dimethylformamide, acetonitrile, ethanol on cytochrome c redox chemistry [71] have been reported. In these publications, the hydrogen bonding interaction is correlated with a change in free energy and solvation energy. Yee at al [72], in their detailed survey of the ligand effect on the reaction entropy of transition metal complexes, noted the possible contribution of outer sphere solvent structuring to the large reorganization energies observed in electron transfer reactions associated with the redox chemistry of aquo complexes.

In terms of comparison of pure PC and pure water conditions, the much larger value of $D_{[Ru(CN)_6]^{4-}}$ in water (Table 1) has been attributed to the significantly lower viscosity of water. However, the progressive increase in $D_{[Ru(CN)_6]^{4-}}$ by a factor of almost 1.5 for $[Ru(CN)_6]^{4-}$ (Table 2) on addition of up to 1.87 M water to PC is greater than predicted by the decrease in viscosity as discussed above. Furthermore, D_{Fc} remains constant at $3.30 \pm 0.04 \times 10^{-6}$ cm^2 s^{-1} (Table 3 and Fig. S5) and hence is independent of water concentration under the same conditions. On this basis, it is concluded that a change of viscosity of PC is only a minor contributor to the change in mass transport for $[Ru(CN)_6]^{4-}$ in the presence of up to 1.87 M water. The strong interaction between $[Ru(CN)_6]^{4-}$ and water molecules results in a decrease in charge density. Consequently, the extent of ion-pairing and hence the decrease in hydrodynamic radius of $[Ru(CN)_6]^{4-}$ is probably the major reason for the larger increase in $D_{[Ru(CN)_6]^{4-}}$ on addition of water than predicted on the basis of the change in viscosity. Thus the outcome is still in accordance with the Stokes-Einstein relationship (Eq.7).

447 Finally with respect to analysis of DC voltammetry, it is noted that ΔE_p for the $[Ru(CN)_6]^{4-/3-}$
448 process, decreases on addition of water implying a progressive water concentration dependent
449 increase in k^0. In contrast, for the $Fc^{0/+}$ one, ΔE_p remains constant at about 60 mV (Table 3) as
450 expected for a process that is reversible in PC and remains reversible on addition of water on the
451 DC cyclic voltammetric time scale.

452 **3.2 FTAC voltammetric study of the electrode kinetics for the $[Ru(CN)_6]^{4-/3-}$ process at a GC**
453 **electrode in PC (0.10 M Bu_4NPF_6) in the absence and presence of water and in neat water**
454 **(0.10 M KCl)**

455 In principle, the electrode kinetics (k^0 and α values) of the $[Ru(CN)_6]^{4-/3-}$ process in PC with
456 different concentrations of water could be parameterised by undertaking DC cyclic voltammetric
457 experiments over a range of scan rates (timescales) and comparing the data with that derived from
458 simulation. However, there are significant advantages in using the kinetically more sensitive
459 technique of FTAC voltammetry where data collected from a single experiment provide the
460 information over a wide range of timescales [45, 51, 73].
461 For kinetic analysis, it was assumed that complexation reactions involving water are reversible.
462 Thus, the square reaction scheme (Eq.9) can be simplified as in Eq.11 [67]

463 $$Ru^{III} + e^- \rightleftharpoons Ru^{II} \qquad \textbf{(11)}$$

464 where, Ru^{III} and Ru^{II} represent all Ru^{III} and Ru^{II} species present in the solution. The k^0 and α values
465 for the $Ru^{II/III}$ process in PC (0.10 M *n*-Bu_4NPF_6) were determined from analysis of data obtained
466 at a GC electrode using a sine wave perturbation with ΔE = 80 mV and f = 9.02 Hz after confirming

467 that the k^0 value is well below the reversible limit (Fig. 4h) when employing the sixth AC harmonic
468 for data analysis based on the Butler-Volmer relationship [29].

469 Figs. 4(a-g) provide a comparison of experimental and simulated data obtained for the aperiodic
470 DC and fundamental to sixth AC harmonic components from heuristically determined best fit
471 values for the $[Ru(CN)_6]^{4-/3-}$ process in neat PC (0.10 M *n*-Bu_4NPF_6) at a GC electrode. In this
472 exercise, only k^0 and α values were determined with the value of $E^0_{f,PC}$ being that derived from
473 analysis of the DC cyclic voltammetric data. Agreement between simulated and experimental data
474 in neat PC (0.10 M *n*-Bu_4NPF_6) is excellent as also is the case on addition of water. Examination
475 of Figs. 4a and 4b shows that the background capacitance current is substantial in the aperiodic
476 DC and fundamental harmonic AC components but essentially absent in the higher order second
477 to sixth AC harmonics. The fourth harmonic components of FTAC voltammograms obtained in
478 PC in the presence of different amount of water are presented in Figs. 5a and 5b and show the
479 expected shift in potential as well as an increase in current on addition of water. The latter effect
480 is accounted for by both an increase in D (see Table 2) and by an increase in k^0. As shown by
481 examination of data in Table 4, $k^0_{PC+\,H_2O}$ in PC increases slightly in the presence of up to 1.87 M
482 water, but the effect is not as dramatic as with changes in $E^0_{f,PC\quad H_2O}$. In neat water containing 0.10
483 M KCl, a k^0 value of 0.19 cm s^{-1} was extracted from simulation of FTAC voltammetric data
484 obtained at a GC electrode for 0.81 mM $[Ru(CN)_6]^{4-}$ with ΔE = 80 mV and f = 80.99 Hz (Fig. 6).

A higher frequency was used in neat water study to provide adequate kinetic sensitivity for the determination of the faster rate of electron transfer.

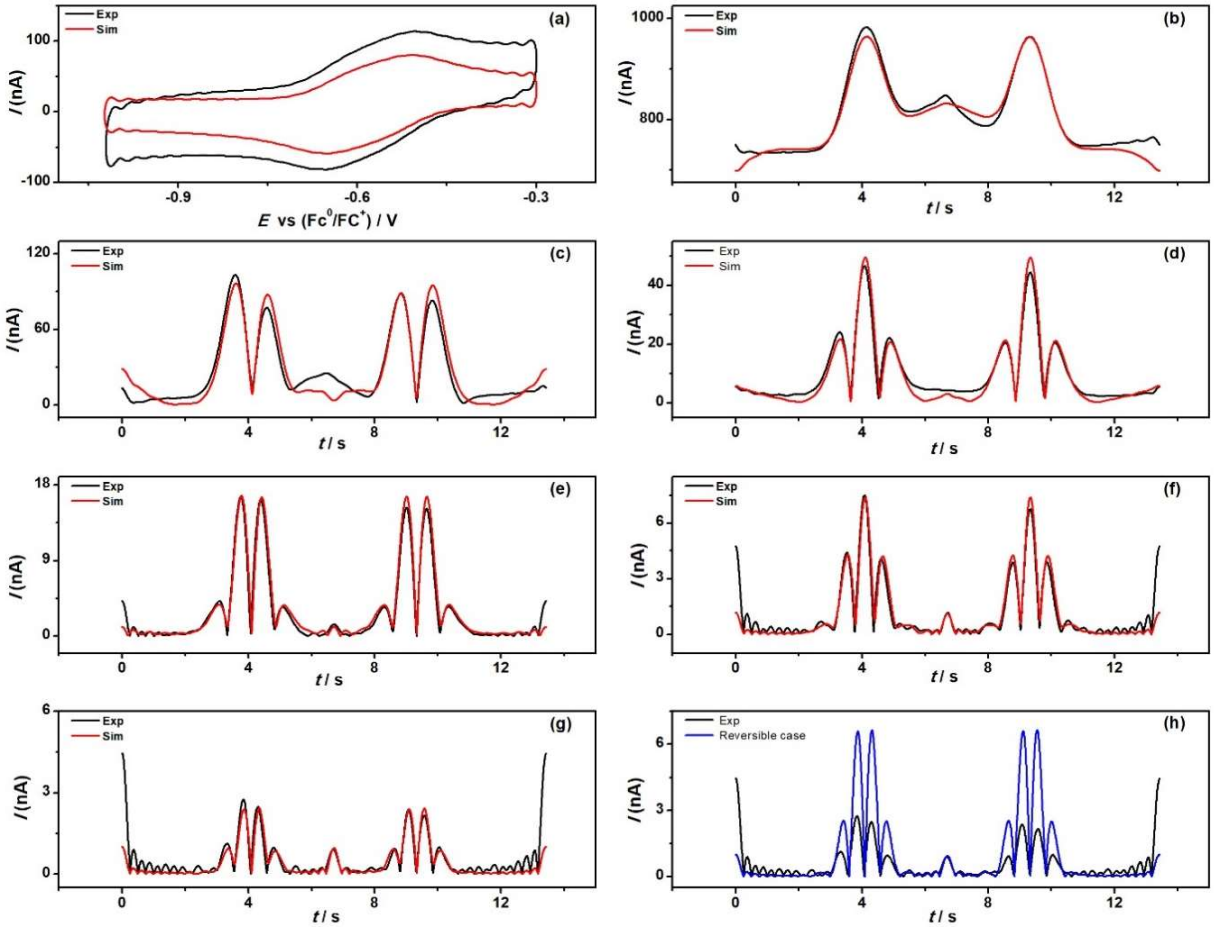

Figure 4: Outcome of heuristic comparison of simulated (red) and experimental (black) FTAC voltammetric data for the $[Ru(CN)_6]^{4-/3-}$ process obtained for the oxidation of 0.083 mM $[Ru(CN)_6]^{4-}$ in PC (0.10 M *n*-Bu_4NPF_6) at a GC electrode (1.0 mm diameter) with ΔE = 80 mV, f = 9.02 Hz and v = 0.108 V s^{-1} **(a)** aperiodic DC component; **(b-g)** 1st- 6th AC harmonic components; **(h)** 6th harmonic for a reversible case (blue) is shown for comparison. Simulated data were obtained with $E^0_{f,PC+H_2O}$ = -656 mV, k^0 = 1.81 x 10^{-2} cm s^{-1}, α_{PC+H_2O} = 0.50, R_u = 2828 Ω, D = 1.91 × 10^{-6} cm^2 s^{-1}.

Figs. 5c and 5d provide plots of $D_{[Ru(CN)_6]^{4-}}$ and $k^0_{PC\ \ H_2O}$ for the $[Ru(CN)_6]^{4-/3-}$ process as a function of $\log_{10}$ [H_2O], respectively. A correlation of these mass transport and electrode kinetic parameters with respect to water concentration is indicated.

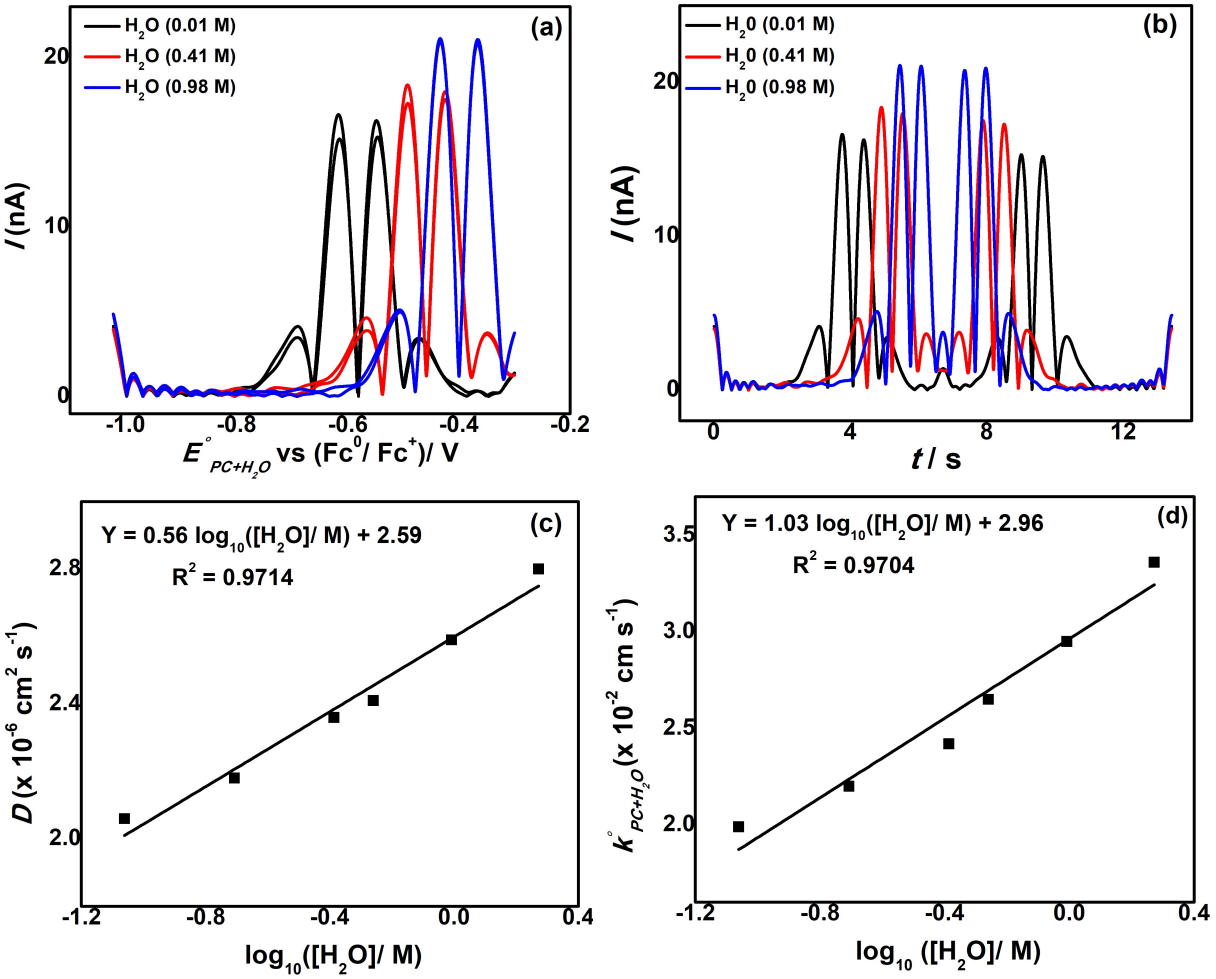

Figure 5: 4th harmonic components of FTAC voltammograms obtained at a GC electrode for the $[Ru(CN)_6]^{4-/3-}$ process in PC (v = 0.108 V s^{-1}) with 0.10 M n-Bu_4NPF_6 as supporting electrolyte with designated water concentrations (a) current versus potential scale, (b) current versus time scale, (c) plot of $D_{[Ru(CN)_6]^{4-}}$ *vs* water concentration (d) plot of $k^0_{PC+H_2O}$ for the $[Ru(CN)_6]^{4-/3-}$ process *vs* water concentration.

Table 4: Summary of data obtained by heuristic analysis of FTAC voltammetry at GC electrode for the $[Ru(CN)_6]^{4-/3-}$ process in PC in the presence of designated amount of water using 0.10 M *n*-Bu_4NPF_6 as supporting electrolyte. ΔE = 80 mV, f = 9.02 Hz and v = 0.108 V s^{-1}.

Water conc. (M)	**Ru (Ω)**	C_{dl} **(μF)**	$E^0_{f,PC+H_2O}$ *vs* $Fc^{0/+}$ **(V)**	$\Delta E^0_{f,PC+H_2O}$ **(mV)**	$k^0_{PC+H_2O}$ **(10^{-2} cm s^{-1})**	α
0.01	2828	19.7, 1.25, 6.96, 3.96, -21.8	-0.656	0	1.81	0.50
0.09	2821	20.3, 0.51, 6.32, 7.14, -0.15	-0.588	68	2.00	0.49
0.20	2806	21.8, 0.59, 6.42, 9.23, -1.66	-0.524	132	2.20	0.49
0.41	2793	22.1, 1.40, 7.80, 4.04, -15.6	-0.462	194	2.40	0.51
0.55	2778	19.6, 0.28, 9.80, 3.41, -19.5	-0.428	228	2.65	0.52
0.98	2756	22.1, 1.45, 7.82, 4.00, -15.0	-0.363	293	2.95	0.49
1.87	2706	15.8, 17.6, -24.0, 9.6, 20.30	-0.301	355	3.38	0.52

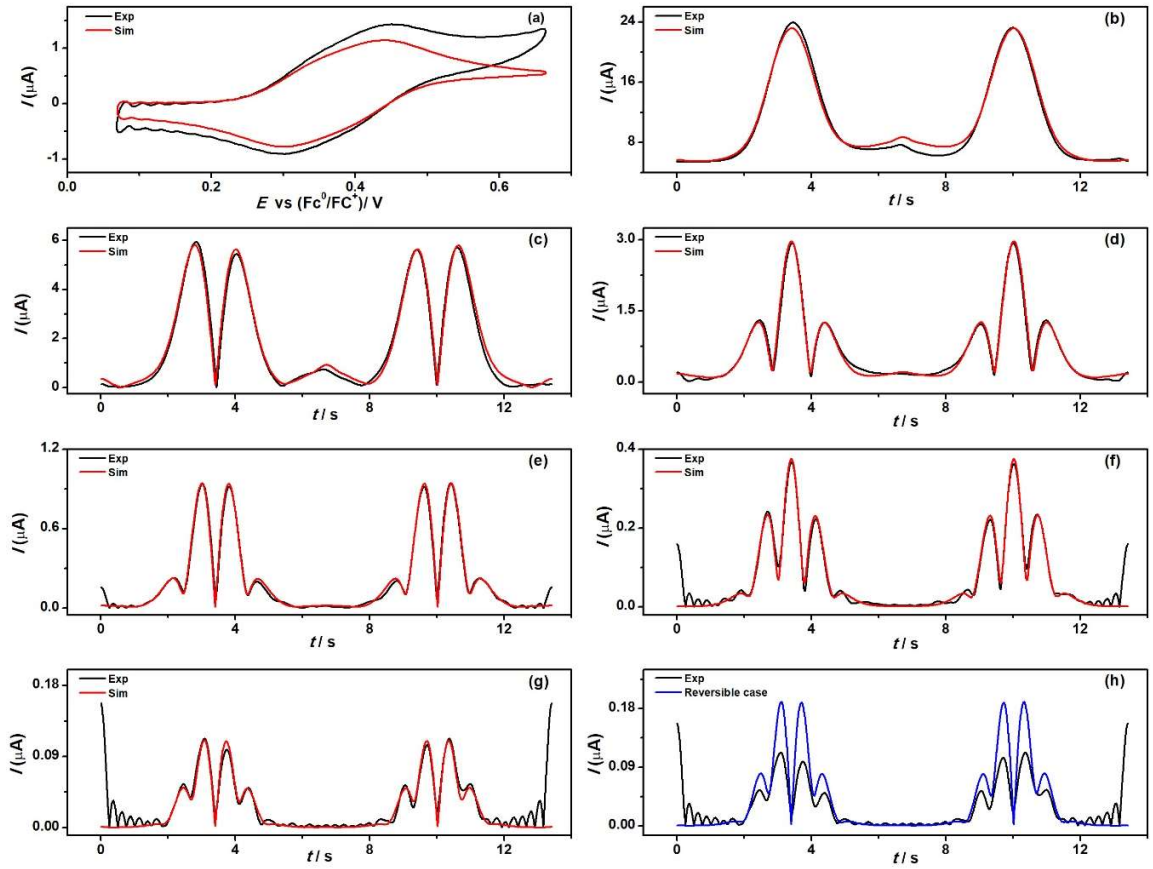

Figure 6: Outcome of heuristic comparison of simulated (red) and experimental (black) FTAC voltammetric data for the $[Ru(CN)_6]^{4-/3-}$ process obtained for the oxidation of 0.81 mM $[Ru(CN)_6]^{4-}$ in aqueous media (0.10 M KCl) at a GC electrode (1.0 mm diameter) with ΔE = 80 mV, f = 80.99 Hz and v = 0.089 V s^{-1} **(a)** aperiodic DC component; **(b-g)** 1st- 6th AC harmonic components; **(h)** 6th harmonic for a reversible case (blue) is shown for comparison. Simulated data were obtained with E^0_{f,H_2O} = -340 mV, k^0 = 0.19 cm s^{-1}, α_{H_2O} = 0.53, R_u = 328 Ω, D = 6.91 × 10^{-6} cm^2 s^{-1}.

In the parametrization of the thermodynamic and electrode kinetics using computer supported data optimization, input parameter ranges were based on the estimations of these parameters made from heuristic analysis. This enables the search of the parameter space to be minimized and saves

substantial computing time. Accordingly, in neat PC the ranges selected were $E^0_{f,PC}$ = -666 to -646 mV (1.0 mV), k^0_{PC} = 1.50 to 2.10 × 10^{-2} cm s^{-1} (0.01 cm s^{-1}) and α_{PC} = 0.4 to 0.6 (0.01) with the resolution given in parenthesis and other input parameters (C, R_u and D) used in the automated data optimization were the same as in the heuristic analysis. In neat water, the ranges selected were E^0_{f,H_2O} = 330 to 350 mV (1.0 mV), $k^0_{H_2O}$ = 0.15 to 0.25 cm s^{-1} (0.01 cm s^{-1}) and α_{H_2O} = 0.4 to 0.6 (0.01) with the resolution given in parenthesis. The optimal fits achieved via this approach are presented in Figs. S6 and S7. The data corresponding to the best fits using the second to sixth AC harmonic components, are summarized in Tables S1 and S2 along with the LS values. The parameters deduced by the heuristic and computational based data optimization forms of analysis are in excellent agreement.

Ion-pairing with the electrolyte (0.10 M *n*-Bu_4NPF_6) could have an impact on the electrode kinetics[67, 74] as well as thermodynamics. However, since the dielectric constant of 64.9 for PC at 25 ºC [75] is not greatly different to that of 78 for water at 25 ºC [76], modification of ion-pairing in PC and hence impact on k^0 upon addition of water are not expected to be large.

According to the Marcus Theory of electron transfer, k^0 associated with a simple outer sphere electrode process is expected to decrease when the solvent viscosity increases [30, 77-79]. Changes in the value of k^0 for the $[Ru(CN)_6]^{4-/3-}$ process correlate qualitatively with differences in viscosity in neat PC and water solvents. Other observations also can be considered in terms of Marcus theory. For example, in this study, in terms of the thermodynamics, the equivalent of the transfer of four water molecules occurs in the secondary coordination sphere when $[Ru(CN)_6]^{4-}$ is oxidized to $[Ru(CN)_6]^{3-}$. This enhanced reorganization effect could in principle lead to a decrease in the k^0

551 value on addition of water. However, k^0 increases slightly when water is added to PC. This
552 apparently contradictory result may be a result of a double layer effect [30], which should enhance
553 k^0 due to a positive shift in E_f^0, and hence compensate for the decrease in k^0 due to solvent
554 reorganization. The data of Noftle and Pletcher [31] imply that the extent of water reorganisation is
555 even larger for the $[Fe(CN)_6]^{4-/3-}$ process (six versus four water molecules transferred). This may
556 provide a rationalisation for the smaller k^0 value of 0.10 cm s^{-1} for the $[Fe(CN)_6]^{4-/3-}$ process [80]
557 than the value of 0.19 cm s^{-1} found herein for the $[Ru(CN)_6]^{4-/3-}$ process at a GC electrode in
558 aqueous 0.10 M KCl electrolyte media. However, caution is needed with this interpretation as
559 neither k^0 value has been corrected for double layer effects [30], nor have ion-pairing differences
560 been considered. Finally, use of concepts based on the Marcus model for an outer sphere process
561 is problematic, as $[Ru(CN)_6]^{4-/3-}$ process is inherently complex. Nevertheless, it is noteworthy that
562 the change in k^0 for the $[Ru(CN)_6]^{4-/3-}$ process is logarithmically related to the shift in E_f^0 in the
563 presence of up to 1.87 M water (Fig. 7).
564
565
566
567
568
569
570

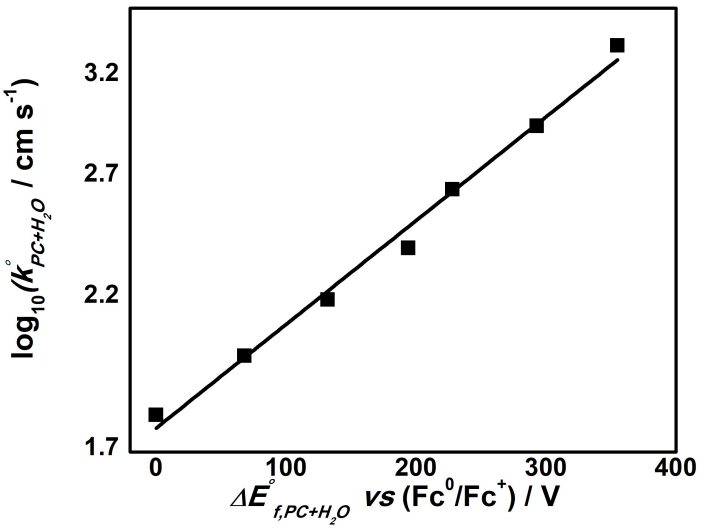

Figure 7: A plot of $\log_{10}(k^0_{PC+H_2O})$ versus $\Delta E^0_{f,PC+\,H_2O}$ with different water concentrations (0.01, 0.09, 0.20, 0.41, 0.55, 0.98, 1.87 M, bottom to top).

4. Conclusion

Parameterisation of E^0, k^0, α and $D_{[Ru(CN)_6]^{4-}}$ values that respectively quantify the thermodynamics, electron transfer kinetics and diffusivity associated with $[Ru(CN)_6]^{4-/3-}$ process has been undertaken at a GC electrode in PC (0.10 M *n*-Bu_4NPF_6) without and with addition of low concentrations of water and in purely aqueous 0.10 M KCl electrolyte using DC and FTAC voltammetry. For this process, $E^0_{f,PC+\,H_2O}$ progressively becomes about 350 mV more positive than $E^0_{f,PC}$ on addition of up to 1.87 M of water and in fully aqueous media the positive shift is about 1.0 V. The E^0_f shifts observed on addition of water can be modelled by assuming that the equivalent of four water molecules hydrogen bonded to the terminal N group of the cyanide ligand are transferred in the secondary coordination sphere when $[Ru(CN)_6]^{4-}$ is oxidised to $[Ru(CN)_6]^{3-}$ versus six in an earlier related study by Noftle and Pletcher [31] on the $[Fe(CN)_6]^{3-/4-}$ process. In contrast to the large positive shifts in E^0_f, only modest increases in k^0 and $D_{[Ru(CN)_6]^{4-}}$ were found on addition of up to 1.87 M water. Some aspects of the electrode kinetic effects are qualitatively in agreement with predictions based on Marcus theory. The fact that E^0_f for the $Fc^{0/+}$ process in PC remained almost unchanged on addition of low concentrations of water implies that detection of large solvent effects on this parameter requires strongly coupled electron transfer and solvent interactions as present in the $[Ru(CN)_6]^{3-/4-}$ process. Finally, it is noted that enhanced values in $D_{[Ru(CN)_6]^{4-}}$ and k^0 are not predominantly due to the decrease in viscosity that occurs on addition of up to 1.87 M water to PC.

ASSOCIATED CONTENT

Supporting information

The Electronic Supplementary information has been submitted as a separate file.

ATR FT-IR spectra of ruthenium complexes, cyclic voltammetry of ruthenium cyanide in PC and aqueous media and the effect of added PC on its voltammetric characteristics in aqueous media, effect of added water on the diffusion coefficient of ferrocene in PC, FTAC voltammogram of ruthenium cyanide in PC and aqueous media, and comparison of parameters derived from the heuristic and automated computer assisted methods of data analysis.

AUTHOR INFORMATION

Corresponding Authors

Associate Professor Jie Zhang- *School of Chemistry, Monash University, Clayton, VIC, 3800, Australia, ARC Centre of Excellence for Electromaterials Science, Monash University, Clayton, VIC 3800, Australia*

Orcid- orcid.org/0000-0003-2493-5209

Email- jie.zhang@monash.edu

Professor Alan Bond- *School of Chemistry, Monash University, Clayton, VIC, 3800, Australia, ARC Centre of Excellence for Electromaterials Science, Monash University, Clayton, VIC 3800, Australia*

Orcid- orcid.org/0000-0002-1113-5205

Email- alan.bond@monash.edu

Authors

Atul Sharma- *School of Chemistry, Monash University, Clayton, VIC, 3800, Australia*

Orcid- orcid.org/0000-0003-0877-1275

Jiezhen Li- *School of Chemistry, Monash University, Clayton, VIC, 3800, Australia*

Si-Xuan Guo- *School of Chemistry, Monash University, Clayton, VIC, 3800, Australia, ARC Centre of Excellence for Electromaterials Science, Monash University, Clayton, VIC 3800, Australia*

Notes

The authors declare no conflict of interest.

ACKNOWLEDGMENTS

The authors acknowledge Rebecca Bac for conducting the Karl Fisher titration experiments and Gareth Kennedy, Anisur Rahman and Luke Gundry for fruitful discussions. JZ and AMB thank the Australian Research Council for financial support.

References:

1. Konezny, S.; D. Doherty, M.; Luca, O.; Crabtree, R.; Soloveichik, G.; Batista, V., *Reduction of Systematic Uncertainty in Dft Redox Potentials of Transition-Metal Complexes*, 2012; Vol. 116, p 6349-6356.
2. Bortolotti, C. A.; Amadei, A.; Aschi, M.; Borsari, M.; Corni, S.; Sola, M.; Daidone, I., The Reversible Opening of Water Channels in Cytochrome C Modulates the Heme Iron Reduction Potential. *J. Am. Chem. Soc.* **2012**, *134*, 13670-13678.
3. Jabłońska-Wawrzycka, A.; Rogala, P.; Michałkiewicz, S.; Hodorowicz, M.; Barszcz, B., Ruthenium Complexes in Different Oxidation States: Synthesis, Crystal Structure, Spectra and Redox Properties. *Dalton Trans.* **2013**, *42*, 6092-6101.
4. Schilt, A. A., Formal Oxidation-Reduction Potentials and Indicator Characteristics of Some Cyanide and 2,2 -Bipyridine Complexes of Iron, Ruthenium, and Osmium. *Anal. Chem.* **1963**, *35*, 1599-1602.
5. Wang, P.; Zakeeruddin, S. M.; Moser, J. E.; Humphry-Baker, R.; Comte, P.; Aranyos, V.; Hagfeldt, A.; Nazeeruddin, M. K.; Grätzel, M., Stable New Sensitizer with Improved Light Harvesting for Nanocrystalline Dye-Sensitized Solar Cells. *Adv. Mater.* **2004**, *16*, 1806-1811.
6. Wang, P.; Zakeeruddin, S. M.; Moser, J. E.; Nazeeruddin, M. K.; Sekiguchi, T.; Grätzel, M., A Stable Quasi-Solid-State Dye-Sensitized Solar Cell with an Amphiphilic Ruthenium Sensitizer and Polymer Gel Electrolyte. *Nat. Mater.* **2003**, *2*, 402-407.
7. Zeng, L.; Gupta, P.; Chen, Y.; Wang, E.; Ji, L.; Chao, H.; Chen, Z.-S., The Development of Anticancer Ruthenium(Ii) Complexes: From Single Molecule Compounds to Nanomaterials. *Chem. Soc. Rev.* **2017**, *46*, 5771-5804.
8. Hoddenbagh, J. M. A.; Macartney, D. H., Kinetics of Electron-Transfer Reactions Involving the Hexacyanoruthenate(4-/3-) Couple in Aqueous Media. *Inorg. Chem.* **1990**, *29*, 245-251.
9. Samsonenko, D. G.; Vostrikova, K. E., Effective Preparation of a Variety of Ruthenium and Osmium Cyanides: Valuable Precursors for Molecular Nanomagnets. *Eur. J. Inorg. Chem.* **2016**, *2016*, 1369-1375.
10. Gennett, T.; Milner, D. F.; Weaver, M. J., Role of Solvent Reorganization Dynamics in Electron-Transfer Processes. Theory-Experiment Comparisons for Electrochemical and Homogeneous Electron Exchange Involving Metallocene Redox Couples. *J. Phys. Chem.* **1985**, *89*, 2787-2794.
11. Liu, Y.-P.; Newton, M. D., Solvent Reorganization and Donor/Acceptor Coupling in Electron-Transfer Processes: Self-Consistent Reaction Field Theory and Ab Initio Applications. *J. Phys. Chem.* **1995**, *99*, 12382-12386.
12. Porras Gutiérrez, A. G., et al., Insights into Water Coordination Associated with the Cuii/Cui Electron Transfer at a Biomimetic Cu Centre. *Dalton Trans.* **2014**, *43*, 6436-6445.
13. Dey, A.; Jenney, F. E.; Adams, M. W. W.; Babini, E.; Takahashi, Y.; Fukuyama, K.; Hodgson, K. O.; Hedman, B.; Solomon, E. I., Solvent Tuning of Electrochemical Potentials in the Active Sites of Hipip Versus Ferredoxin. *Science* **2007**, *318*, 1464.
14. Hadt, R. G.; Sun, N.; Marshall, N. M.; Hodgson, K. O.; Hedman, B.; Lu, Y.; Solomon, E. I., Spectroscopic and Dft Studies of Second-Sphere Variants of the Type 1 Copper Site in Azurin: Covalent and Nonlocal Electrostatic Contributions to Reduction Potentials. *J. Am. Chem. Soc.* **2012**, *134*, 16701-16716.
15. Marshall, N. M.; Garner, D. K.; Wilson, T. D.; Gao, Y.-G.; Robinson, H.; Nilges, M. J.; Lu, Y., Rationally Tuning the Reduction Potential of a Single Cupredoxin Beyond the Natural Range. *Nature* **2009**, *462*, 113-116.

16. Dey, S.; Rana, A.; Dey, S. G.; Dey, A., Electrochemical Hydrogen Production in Acidic Water by an Azadithiolate Bridged Synthetic Hydrogenese Mimic: Role of Aqueous Solvation in Lowering Overpotential. *ACS Catal.* **2013**, *3*, 429-436.
17. Le Poul, N., et al., Gating the Electron Transfer at a Monocopper Centre through the Supramolecular Coordination of Water Molecules within a Protein Chamber Mimic. *Chem. Sci.* **2018**, *9*, 8282-8290.
18. Samanta, S.; Mittra, K.; Sengupta, K.; Chatterjee, S.; Dey, A., Second Sphere Control of Redox Catalysis: Selective Reduction of O_2 to O_2^- or H_2O by an Iron Porphyrin Catalyst. *Inorg. Chem.* **2013**, *52*, 1443-1453.
19. Vergara, M. M.; Posse, M. E. G.; Fagalde, F.; Katz, N. E.; Fiedler, J.; Sarkar, B.; Sieger, M.; Kaim, W., Mixed-Valency with Cyanides as Terminal Ligands: Diruthenium(III,II) Complexes with the 3,6-Bis(2-Pyridyl)-1,2,4,5-Tetrazine Bridge and Variable Co-Ligands (CN^- Vs. bpy or NH_3). *Inorg. Chim. Acta* **2010**, *363*, 163-167.
20. Wragg, A. B.; Derossi, S.; Easun, T. L.; George, M. W.; Sun, X.-Z.; Hartl, F.; Shelton, A. H.; Meijer, A. J. H. M.; Ward, M. D., Solvent-Dependent Modulation of Metal–Metal Electronic Interactions in a Dinuclear Cyanoruthenate Complex: A Detailed Electrochemical, Spectroscopic and Computational Study. *Dalton Trans.* **2012**, *41*, 10354-10371.
21. Scheiring, T.; Kaim, W.; Olabe, J. A.; Parise, A. R.; Fiedler, J., The Valence-Localized Decacyanodiruthenium(III,II) Analogue of the Creutz–Taube Ion. Completing the Full d^5/d^6 Triad $[(NC)_5M(\mu\text{-pz})M(CN)_5]^{5-}$, M=Fe,Ru,Os; pz=Pyrazine. *Inorg. Chim. Acta* **2000**, *300-302*, 125-130.
22. Derossi, S.; Adams, H.; Ward, M. D., Hydrogen-Bonded Assemblies of Ruthenium(Ii)-Biimidazole Complex Cations and Cyanometallate Anions: Structures and Photophysics. *Dalton Trans.* **2007**, 33-36.
23. Ward, M. D., $[Ru(Bipy)(CN)_4]^{2-}$ and Its Derivatives: Photophysical Properties and Its Use in Photoactive Supramolecular Assemblies. *Coord. Chem. Rev.* **2006**, *250*, 3128-3141.
24. Timpson, C. J.; Bignozzi, C. A.; Sullivan, B. P.; Kober, E. M.; Meyer, T. J., Influence of Solvent on the Spectroscopic Properties of Cyano Complexes of Ruthenium(II). *J. Phys. Chem.* **1996**, *100*, 2915-2925.
25. Arumugam, K.; Becker, U., Computational Redox Potential Predictions: Applications to Inorganic and Organic Aqueous Complexes, and Complexes Adsorbed to Mineral Surfaces. *Minerals* **2014**, *4*, 345.
26. Baik, M.-H.; Friesner, R. A., Computing Redox Potentials in Solution: Density Functional Theory as a Tool for Rational Design of Redox Agents. *J. Phys. Chem. A* **2002**, *106*, 7407-7412.
27. Chiorescu, I.; Deubel, D. V.; Arion, V. B.; Keppler, B. K., Computational Electrochemistry of Ruthenium Anticancer Agents. Unprecedented Benchmarking of Implicit Solvation Methods. *J. Chem. Theory Comput.* **2008**, *4*, 499-506.
28. Tsai, M.-K.; Rochford, J.; Polyansky, D. E.; Wada, T.; Tanaka, K.; Fujita, E.; Muckerman, J. T., Characterization of Redox States of $Ru(OH_2)(Q)(tpy)^{2+}$ (Q = 3,5-di-tert-butyl-1,2-benzoquinone, tpy = 2,2′:6′,2″-terpyridine) and Related Species through Experimental and Theoretical Studies. *Inorg. Chem.* **2009**, *48*, 4372-4383.
29. Butler, J. A. V., Studies in Heterogeneous Equilibria. Part II.—the Kinetic Interpretation of the Nernst Theory of Electromotive Force. *Trans. Faraday Soc.* **1924**, *19*, 729-733.
30. Allen J. Bard and Larry R. Faulkner, Electrochemical Methods: Fundamentals and Applications, New York: Wiley, 2001, 2nd Ed. *Russ. J. Electrochem.* **2002**, *38*, 1364-1365.
31. Noftle, R. E.; Pletcher, D., An Interpretation of the Formal Potential for the Ferricyanide / Ferrocyanide Couple as a Function of Solvent Composition. *J. Electroanal. Chem. Interfacial Electrochem.* **1990**, *293*, 273-277.
32. Hush, N. S., Adiabatic Rate Processes at Electrodes. I. Energy-Charge Relationships. *J. Chem. Phys.* **1958**, *28*, 962-972.

33. Marcus, R. A., On the Theory of Oxidation-Reduction Reactions Involving Electron Transfer. *J. Chem. Phys.* **1956**, *24*, 966-978.
34. Fujinaga, T.; Izutsu, K., Propylene Carbonate. In *Recommended Methods for Purification of Solvents and Tests for Impurities*, Coetzee, J. F., Ed. Pergamon: 1982; pp 19-24.
35. Ginsberg, A. P.; Koubek, E. Y., Hydrogen Bonding in Ferrocyanic, Ruthenocyanic, and Osmocyanic Acids. *Inorg. Chem.* **1965**, *4*, 1186-1194.
36. Vogler, A.; Kunkely, H., Photochemical Redox Decomposition of μ-cyano-pentacyanoruthenium (II)pentaamminecobalt(III) Ion. *Ber. Bunsenges. Phys. Chem.* **1975**, *79*, 83-86.
37. Zaldivar, G. A. P.; Gushikem, Y.; Kubota, L. T., Tin(IV) Oxide Grafted on a Silica Gel Surface as a Conducting Substrate Base for Cupric Hexacyanoferrate. *J. Electroanal. Chem. Interfacial Electrochem.* **1991**, *318*, 247-254.
38. Coates, J., Interpretation of Infrared Spectra, A Practical Approach. In *Encyclopedia of Analytical Chemistry*; Meyers R. A. and Mckelvy M. L. Eds.; Wiely: 2006.
39. Gritzner, G.; Kuta, J., Recommendations on Reporting Electrode Potentials in Nonaqueous Solvents (Recommendations 1983). *Pure Appl. Chem.* **1984**, *56*, 461-466.
40. Gagne, R. R.; Koval, C. A.; Lisensky, G. C., Ferrocene as an Internal Standard for Electrochemical Measurements. *Inorg. Chem.* **1980**, *19*, 2854-2855.
41. Pavlishchuk, V. V.; Addison, A. W., Conversion Constants for Redox Potentials Measured Versus Different Reference Electrodes in Acetonitrile Solutions at 25°C. *Inorg. Chim. Acta* **2000**, *298*, 97-102.
42. Zhang, J.; Guo, S.-X.; Bond, A. M., Discrimination and Evaluation of the Effects of Uncompensated Resistance and Slow Electrode Kinetics from the Higher Harmonic Components of a Fourier Transformed Large-Amplitude Alternating Current Voltammogram. *Anal. Chem.* **2007**, *79*, 2276-2288.
43. Zoski, C. G.; Bond, A. M.; Colyer, C. L.; Myland, J. C.; Oldham, K. B., Near-Steady-State Cyclic Voltammetry at Microelectrodes. *J. Electroanal. Chem. Interfacial Electrochem.* **1989**, *263*, 1-21.
44. Li, J.; Guo, S.-X.; Bentley, C. L.; Bano, K.; Bond, A. M.; Zhang, J.; Ueda, T., Electrode Material Dependence of the Electron Transfer Kinetics Associated with the $[SVW_{11}O_{40}]^{3-/4-}$ ($V^{V/IV}$) and $[SVW_{11}O_{40}]^{4-/5-}$ ($W^{VI/V}$) Processes in Dimethylformamide. *Electrochim. Acta* **2016**, *201*, 45-56.
45. Bond, A. M.; Duffy, N. W.; Guo, S.-X.; Zhang, J.; Elton, D., Changing the Look of Voltammetry. *Anal. Chem.* **2005**, *77*, 186 A-195 A.
46. Adeloye, A. O., Synthesis, Photophysical and Electrochemical Properties of a Mixed bipyridyl-phenanthrolyl Ligand Ru(II) Heteroleptic Complex Having trans-2-methyl-2-butenoic acid Functionalities. *Molecules* **2011**, *16*, 8353-8367.
47. Morris, L. K.; Abu, E. A.; Bowman, C.; Estridge, C. E.; Andria, S. E.; Seliskar, C. J.; Heineman, W. R., Effect of the Concentration of Supporting Electrolyte on Spectroelectrochemical Detection of [Ru(Bpy)3]2+. *Electroanalysis* **2011**, *23*, 939-946.
48. Zhang, Y.; Simonov, A. N.; Zhang, J.; Bond, A. M., Fourier Transformed Alternating Current Voltammetry in Electromaterials Research: Direct Visualisation of Important Underlying Electron Transfer Processes. *Curr. Opin. Electrochem.* **2018**, *10*, 72-81.
49. Li, J.; Bentley, C. L.; Ueda, T.; Bond, A. M.; Zhang, J., Electrolyte Cation Dependence of the Electron Transfer Kinetics Associated with the $[SVW_{11}O_{40}]^{3-/4-}$ ($V^{V/IV}$) and $[SVW_{11}O_{40}]^{4-/5-}$ ($W^{VI/V}$) Processes in Propylene Carbonate. *J. Electroanal. Chem.* **2018**, *819*, 193-201.
50. Tokuda, K.; Matsuda, H., Theory of A.C. Voltammetry at a Rotating Disk Electrode: Part I. A Reversible Electrode Process. *J. Electroanal. Chem. Interfacial Electrochem.* **1977**, *82*, 157-171.
51. Kennedy, G. F.; Bond, A. M.; Simonov, A. N., Modelling Ac Voltammetry with Mecsim: Facilitating Simulation–Experiment Comparisons. *Curr. Opin. Electrochem.* **2017**, *1*, 140-147.

52. Miller, C. C.; Walker, J., The Stokes-Einstein Law for Diffusion in Solution. *P. Roy. Soc. A - Math. Phys.* **1924**, *106*, 724-749.
53. O'Mullane, A. P.; Macpherson, J. V.; Unwin, P. R.; Cervera-Montesinos, J.; Manzanares, J. A.; Frehill, F.; Vos, J. G., Measurement of Lateral Charge Propagation in $[Os(bpy)_2(pvp)NCl]Cl$ Thin Films: A Scanning Electrochemical Microscopy Approach. *J. Phys. Chem. B* **2004**, *108*, 7219-7227.
54. Feng, G.; Xiong, Y.; Wang, H.; Yang, Y., Cyclic Voltammetry Investigation of Diffusion of Ferrocene within Propylene Carbonate Organogel Formed by Gelator. *Electrochim. Acta* **2008**, *53*, 8253-8257.
55. Janisch, J.; Ruff, A.; Speiser, B.; Wolff, C.; Zigelli, J.; Benthin, S.; Feldmann, V.; Mayer, H. A., Consistent Diffusion Coefficients of Ferrocene in Some Non-Aqueous Solvents: Electrochemical Simultaneous Determination Together with Electrode Sizes and Comparison to Pulse-Gradient Spin-Echo Nmr Results. *J. Solid State Electrochem.* **2011**, *15*, 2083.
56. Courtot, C.; L'her, M., Proprietes Physiques Des Melanges Eau-Carbonate De Propylene a 25 °C. C.R. Acad. Sc. Paris **1972**, *275*, 195-198.
57. Gutmann, V., Empirical Parameters for Donor and Acceptor Properties of Solvents. *Electrochim. Acta* **1976**, *21*, 661-670.
58. Kolling, O. W., Comparison of Donor-Acceptor Parameters in Nonaqueous Solvents. *Analy. Chem.* **1982**, *54*, 260-264.
59. Gritzner, G.; Danksagmüller, K.; Gutmann, V., Outer-Sphere Coordination Effects on the Redox Behaviour of the $Fe(CN)_6^{3-}/Fe(CN)_6^{4-}$ Couple in Non-Aqueous Solvents. *J. Electroanal. Chem. Interfacial Electrochem.* **1976**, *72*, 177-185.
60. Gritzner, G.; Danksagmüller, K.; Gutmann, V., Solvent Effects on the Redox Potentials of Tetraethylammonium Hexacyanomanganate(III) and Hexacyanoferrate(III). *J. Electroanal. Chem. Interfacial Electrochem.* **1978**, *90*, 203-210.
61. Gutmann, V.; Gritzner, G.; Danksagmuller, K., Solvent Effects on the Redox Potential of Hexacyanoferrate(III)-Hexacyanoferrate(II). *Inorg. Chim. Acta* **1976**, *17*, 81-86.
62. Heyrovský, J.; Kůta, J., I - Principles of Polarography. In *Principles of Polarography*, Heyrovský, J.; Kůta, J., Eds. Academic Press: 1965; pp 17-34.
63. Meites, L., Polarographic Techniques. *Interscience: New York.* **1965;** pp267-284.
64. Rahman, M. A.; Li, J.; Guo, S.-X.; Kennedy, G.; Ueda, T.; Bond, A. M.; Zhang, J., Modelling Limitations Encountered in the Thermodynamic and Electrode Kinetic Parameterization of the A-$[S_2W_{18}O_{62}]^{4-/5-/6-}$ Processes at Glassy Carbon and Metal Electrodes. *J. Electroanal. Chem.* **2019**, 113786.
65. Peruzzi, N.; Lo Nostro, P.; Ninham, B.; Baglioni, P., The Solvation of Anions in Propylene Carbonate. *J. Solu. Chem.* **2015**, *44*.
66. Soetens, J.-C.; Millot, C.; Maigret, B., Molecular Dynamics Simulation of $Li^+BF_4^-$ in Ethylene Carbonate, Propylene Carbonate, and Dimethyl Carbonate Solvents. *J. Phys. Chem. A* **1998**, *102*, 1055-1061.
67. Liu, Y. P.; Guo, S. X.; Bond, A. M.; Zhang, J.; Geletii, Y. V.; Hill, C. L., Voltammetric Determination of the Reversible Potentials for $[\{Ru_4O_4(OH)_2(H_2O)_4\}(\gamma\text{-}SiW_{10}O_{36})_2]^{10-}$ over the pH Range of 2-12: Electrolyte Dependence and Implications for Water Oxidation Catalysis. *Inorg. Chem.* **2013**, *52*, 11986-11996.
68. Battistuzzi, G.; Borsari, M.; Rossi, G.; Sola, M., Effects of Solvent on the Redox Properties of Cytochrome C: Cyclic Voltammetry and ^1H NMR Experiments in Mixed Water-Dimethylsulfoxide Solutions. *Inorg. Chim. Acta* **1998**, *272*, 168-175.
69. Peover, M. E.; Powell, J. S., Dependence of Electrode Kinetics on Molecular Structure Nitro-Compounds in Dimethylformamide. *J. Electroanal. Chem. Interfacial Electrochem.* **1969**, *20*, 427-433.

70. Gupta, N.; Linschitz, H., Hydrogen-Bonding and Protonation Effects in Electrochemistry of Quinones in Aprotic Solvents. *J. Am. Chem. Soc.* **1997**, *119*, 6384-6391.
71. Borsari, M.; Bellei, M.; Tavagnacco, C.; Peressini, S.; Millo, D.; Costa, G., Redox Thermodynamics of Cytochrome C in Mixed Water–Organic Solvent Solutions. *Inorg. Chim. Acta* **2003**, *349*, 182-188.
72. Yee, E. L.; Cave, R. J.; Guyer, K. L.; Tyma, P. D.; Weaver, M. J., A Survey of Ligand Effects Upon the Reaction Entropies of Some Transition Metal Redox Couples. *J. Am. Chem. Soc.* **1979**, *101*, 1131-1137.
73. Bond, A. M.; Elton, D.; Guo, S.-X.; Kennedy, G. F.; Mashkina, E.; Simonov, A. N.; Zhang, J., An Integrated Instrumental and Theoretical Approach to Quantitative Electrode Kinetic Studies Based on Large Amplitude Fourier Transformed A.C. Voltammetry: A Mini Review. *Electrochem. Commun.* **2015**, *57*, 78-83.
74. Guo, S. X.; Feldberg, S. W.; Bond, A. M.; Callahan, D. L.; Richardt, P. J. S.; Wedd, A. G., Systematic Approach to the Quantitative Voltammetric Analysis of the Fe^{III}/Fe^{II} Component of the $[\alpha_2\text{-}Fe(OH_2)P_2W_{17}O_{61}]^{7-/8-}$ Reduction Process in Buffered and Unbuffered Aqueous Media. *J. Phys. Chem. B* **2005**, *109*, 20641-20651.
75. Barthel, J.; Feuerlein, F., Dielectric Properties of Propylene Carbonate and Propylene Carbonate Solutions. *J. Solu. Chem.* **1984**, *13*, 393-417.
76. Malmberg, C.; Maryott, A., Dielectric Constant of Water from 0 °C to 100 °C. *J. Res. Natl. Inst. Stand. Technol.* **1956**, *56*, 1.
77. Lagrost, C.; Preda, L.; Volanschi, E.; Hapiot, P., Heterogeneous Electron-Transfer Kinetics of Nitro Compounds in Room-Temperature Ionic Liquids. *J. Electroanal. Chem.* **2005**, *585*, 1-7.
78. Bentley, C. L.; Li, J.; Bond, A. M.; Zhang, J., Mass-Transport and Heterogeneous Electron-Transfer Kinetics Associated with the Ferrocene/Ferrocenium Process in Ionic Liquids. *J. Phys. Chem. C* **2016**, *120*, 16516-16525.
79. Rubinstein, I., *Physical Electrochemistry: Science and Technology*; CRC Press, 1995; Vol. 7.
80. Sher, A. A.; Bond, A. M.; Gavaghan, D. J.; Harriman, K.; Feldberg, S. W.; Duffy, N. W.; Guo, S.-X.; Zhang, J., Resistance, Capacitance, and Electrode Kinetic Effects in Fourier-Transformed Large-Amplitude Sinusoidal Voltammetry: Emergence of Powerful and Intuitively Obvious Tools for Recognition of Patterns of Behavior. *Anal. Chem.* **2004**, *76*, 6214-6228.

842 **Graphical abstract**